Apoptosis (2019) 24:718–729
https://doi.org/10.1007/s10495-019-01552-w

Fipronil induces apoptosis and cell cycle arrest in porcine oocytes during in vitro maturation

Wenjun Zhou[1] · Ying-Jie Niu[1] · Zheng-Wen Nie[1] · Yong-Han Kim[1] · Kyung-Tae Shin[1] · Jing Guo[2,3] · Xiang-Shun Cui[1]

Published online: 25 June 2019

Abstract

Fipronil (FPN) is a widely used phenylpyrazole pesticide that can kill pests by blocking γ-aminobutyric acid (GABA)-gated chloride channels. In addition, there are lack of studies on the effects of FPN on the female mammalian gametes. In this study, porcine oocytes were used to investigate the effects of FPN on the oocyte maturation process. The results showed that the first polar body extrusion rate significantly decreased (100 μM FPN vs. control, 18.64 ± 2.95% vs. 74.90 ± 1.50%, respectively), and oocytes were arrested at the germinal vesicle stage in 100 μM FPN group. Meanwhile, the FPN caused a significant increase in reactive oxygen species (ROS) levels and severe DNA damage inside the oocytes. Furthermore, apoptosis was enhanced along with decreases in mitochondrial membrane potential, BCL-xL, and the release of cytochrome C in FPN-treated group. Additionally, low CDK1 activity and delayed cyclin B1 degradation during germinal vesicle breakdown were found in the FPN-treated group, which resulted from the activation of ATM-P53-P21 pathway. In conclusion, FPN induces apoptosis and cell cycle arrest in porcine oocyte maturation because of increased ROS levels and DNA damage. This suggests that the FPN in the environment may have potential detrimental effects on the female mammalian reproductive system.

Keywords Fipronil · Porcine · Oocyte maturation · Apoptosis · MPF

Introduction

Fipronil (FPN) is a broad-spectrum and highly effective phenylpyrazole insecticide. It is used in the management of rice culture and control of residential veterinary pests, causing extensive aquatic environmental contamination [1] and drug residues in farm products. In insects, FPN interrupts the normal function of the central nervous system of insects by blocking γ-aminobutyric acid (GABA)-gated chloride channels. FPN has been demonstrated to be less toxic to mammals owing to its higher affinity to insect transmitter receptors compared to those in mammals [2]. Furthermore, it has been reported that exposure to micro molar concentrations of phenylpyrazole insecticides (FPN and its metabolites sulfone and sulfide) induced cytotoxicity in various human somatic cells [3–5]. In addition, FPN causes a disruption in thyroid and testis functions in rats [6, 7] as well as high toxicity in zebrafish and carp [8, 9].

Numerous pesticides are capable of increasing levels of reactive oxygen species (ROS) inside cells and inhibit ROS scavengers, which results in oxidative stress [10]. By inducing oxidative imbalance, ROS damage lipids and proteins on the cell membrane while also disturbing membrane permeability. There has been substantial evidence indicating that increased oxidative stress during pesticide treatment, such as increased lipid peroxidation, diminished mitochondrial function and decreased cytochrome oxidase activity [11–13]. Studies have also reported that FPN can cause oxidative stress in rat sperm and human neuroblastoma SH-SY5Y cells by increasing the cytoplasmic ROS [7, 14].

Electronic supplementary material The online version of this article (https://doi.org/10.1007/s10495-019-01552-w) contains supplementary material, which is available to authorized users.

✉ Jing Guo
guojing880414@163.com

✉ Xiang-Shun Cui
xscui@cbnu.ac.kr

[1] Department of Animal Science, Chungbuk National University, Cheongju, Chungbuk 28644, Republic of Korea

[2] Chongqing Key Laboratory of Human Embryo Engineering, Chongqing 400013, China

[3] Chongqing Reproductive and Genetics Institute, Yu Zhong District, Chongqing 400013, China

In other studies, the previous study [15] demonstrated a genotoxic effect of FPN in the fish, which induced micronucleus. In addition, FPN caused a significant increase in micronuclei, sister chromatid exchange frequency, and DNA damage in vitro as well as in vivo in humans and rats [7, 16, 17]. These results suggested that FPN could cause chromosomal abnormalities or DNA damage in somatic or germ cells of fish and mammals.

ROS such as hydrogen peroxide (H_2O_2), superoxide anions (O_2^-), and hydroxyl radicals (OH–) are known for their ability to damage the cellular membrane, DNA, and proteins [18]. Many studies have focused on the role of ROS and antioxidants in the female reproductive system [19, 20]. A high level of ROS and low anti-oxidant activity in follicular fluid has resulted in reduced pregnancy outcomes by IVF [21, 22]. The excessive ROS can impair the mitochondrial membrane permeability and then reduce the membrane potential and suppress the expression of pro-survival genes, such as *Bcl-2* and *Bcl-xL*, which eventually leads to cellular apoptosis because of the release of cytochrome C and activation of the Caspase cascade [23, 24]. Furthermore, ROS can induce DNA damage, which can be detected by cell cycle checkpoint markers, and eventually cause cell cycle arrest during the transition from the G_1 to S phase (G_1–S), or G_2 to M phase (G_2–M) [25].

Meiosis consist of unique cell divisions that produce haploid germ cells. Oogenesis mainly includes germinal vesicles, germinal vesicle breakdown (GVBD), meiosis I, and meiosis II. The porcine oocytes cannot go through the G2–M transition of the first meiotic division (also called GVBD in oocytes) until the cyclin B1-CDK1 complex (also called MPF) activity increases. During the meiotic cell cycle, the cyclin B1-CDK1 complex in oocytes is first activated at meiosis I, then transiently inactivated after the extrusion of the first polar body, and finally reactivated at meiosis II [26]. During the oocyte maturation, the ROS-induced oxidative stress commonly disrupts the function of mitochondria and the formation of spindles in oocytes [27, 28], which results in poor oocyte quality and thereby affect the formation of the blastocyst [29]. Moreover, the high levels of ROS inside the oocytes can cause DNA damage, which can activate DNA damage checkpoint markers such as ATM, Chk2, and p53, which eventually inhibits the activity of the cyclin B1-CDK1 complex [30, 31]. Finally, oocytes with DNA damage arrest at the GV stage and cause a delay of maturation. In conclusion, the oxidative stress and DNA damage can induce apoptosis and cell cycle arrest in oocytes, which leads to poor quality oocytes. Furthermore, the poor quality of oocytes hampers early embryonic development, therefore affecting the health of the fetus and piglets.

Previously, chicken eggs containing FPN were sold to the European Union and Asian countries in 2017. Furthermore, the accumulation of FPN has genetic toxicity to the rat male reproductive system [16] and can induce apoptosis in mouse hepatic cells by inducing excessive ROS [32]. Until now, no studies of FPN in mammalian oocytes have been performed. Therefore, it is necessary to investigate whether FPN will affect oocyte maturation in pigs as well as the underlying mechanism.

Materials and methods

Unless otherwise indicated, all chemicals were purchased from Sigma (Sigma-Aldrich, St. Louis, MO, USA). The FPN was diluted by dimethyl sulfoxide and stored as 100 mM stock. All animal studies were approved and performed within the guidelines of the Institutional Animal Care and Use Committee (IACUC) of Chungbuk National University, Republic of Korea.

Oocyte collection and in vitro maturation

Porcine ovaries were obtained from a local slaughterhouse. Cumulus oocyte complexes (COCs) with a diameter of 3–6 mm were aspirated from the antral follicles and were selected under a stereo-microscope. Oocytes were selected for further experiments if they had a homogeneous ooplasm and were surrounded by a minimum of three layers of cumulus cells. After three washes in Tyrode lactate Hepes (TL-Hepes), the COCs were transferred into an in vitro maturation (IVM) medium containing TCM-199 (Invitrogen, Carlsbad, CA, USA) supplemented with 10% (v/v) porcine follicular fluid, 1 μg/mL insulin, 75 μg/mL kanamycin, 0.91 mM Na pyruvate, 0.57 mM L-cysteine, 10 ng/mL epidermal growth factor, 0.5 μg/mL follicle-stimulating hormone, and 0.5 μg/mL luteinizing hormone, and were cultured at 38.5 °C in an atmosphere of 5% CO_2 and 100% humidity. Oocyte maturation was induced by culturing approximately 50 COCs in four-well dishes containing 500 μL IVM medium supplemented with various concentrations (0, 30, 50, and 100 μM) of FPN. COCs were cultured up to 44 h based on previous studies [33, 34], oocytes were denuded of their cumulus cells by gentle pipetting in 1 mg/mL hyaluronidase at different maturation times.

Cell cycle analysis

Oocytes were collected after 28 h of IVM for cell cycle analysis. Denuded oocytes were stained with Hoechst 33,342 (10 μg/mL in PBS) for 5 min at RT. After washing, the embryos were mounted onto glass slides and observed under a laser scanning confocal microscope. Oocytes with germinal vesicle were considered as GV stage, those with disappeared germinal vesicle and unaligned chromosomes were considered as GVBD stage, those with chromosomes in

alignment were considered as MI stage, those showing two separated groups of chromosomes near the membrane were considered as anaphase I or telophase I, and those with polar bodies were considered as MII stage [35].

ROS staining

Oocytes (n = 22; 3 replicates) were stained for 15 min in phosphate buffered saline (PBS)/polyvinyl alcohol (PVA) containing 10 µM 2′,7′-dichlorodihydrofluorescein diacetate at 37 °C. After incubation, oocytes were washed three times and then transferred to droplets of PBS covered with paraffin oil in a polystyrene culture dish. The fluorescence signal was captured using an epifluorescence microscope (Nikon Corp., Tokyo, Japan). Quantification of ROS levels was performed by analyzing the fluorescence intensity in oocytes using Image J version 1.44 g software (National Institutes of Health, Bethesda, MD, USA).

Assay of mitochondrial membrane potential (ΔΨm)

IVM oocytes in the different treatments at 44 h were incubated in PBS/PVA containing 2.5 µM 5,5′,6,6′-tetrachloro-1,1′,3,3′-tetraethyl-imidacarbocyanine iodide (JC-1) (Cat #M34152, Invitrogen, Carlsbad, CA, USA) at 38.5 °C in 5% CO_2 for 30 min. Membrane potential was calculated as the ratio of red florescence, which corresponded to activated mitochondria (J-aggregates), to green fluorescence, which corresponded to less-activated mitochondria (J-monomers). Fluorescence was visualized using an epifluorescence microscope (Nikon Corp., Tokyo, Japan).

Quantitative reverse-transcription polymerase chain reaction (qRT-PCR)

Next, qRT-PCR was used to evaluate the gene expression in cumulus cells. First, mRNA from cumulus cells was extracted and cDNA was synthesized with a Dynabeads mRNA Direct Kit (61012, ThermoFisher, Waltham, MA, USA) and a First-Strand Synthesis Kit (6210, LeGene, San Diego, CA, USA) according to the manufacturer's instructions. Next, qRT-PCR was conducted using a KAPA SYBR Green FAST qPCR Kit (KK4602, KAPA Biosystems, Wilmington, MA, USA) according to the manufacturer's instructions on a QuantStudio™ 6 Flex Real-Time PCR System (Applied biosystem, USA). The PCR protocol was as follows: initial denaturation at 95 °C for 3 min; followed by 40 cycles of amplification at 95 °C for 20 s, 60 °C for 20 s, and 72 °C for 30 s; and a final extension 95 °C for 10 s. Primer sets for cumulus cell expansion-related genes are listed in Table 1, and the specificity for the target genes were confirmed using primer BLAST.

Immunofluorescence staining

Oocytes were fixed in 3.7% methanol for 30 min at room temperature (RT) and then transferred to phosphate buffer saline/polyvinyl alcohol (PBS/PVA) medium. Next, oocytes were permeabilized in 0.5% Triton-X100 for 30 min at RT. After 3 washes in PBS/PVA (pH 7.5) for 5 min each, the samples were blocked in 1% BSA for 1 h. The oocytes were incubated with primary antibody at 4 °C overnight. The primary antibodies used were rabbit anti-α tubulin (1:400; Cat: #117K4786, Sigma-Aldrich), rabbit anti-γH2A.X (1:100; Cat: #2577; Cell Signaling Technology), rabbit anti-Bcl-xL (1:100; Cat: 2762; Cell Signaling Technology), rabbit anti-p-ATM (1:100; Cat: 5883S; Cell Signaling Technology), rabbit anti-Caspase 3 (CASP3) (1:100; Cat: 047M4794 V; Sigma-Aldrich), and anti-cytochrome C (1:100; Cat: ab110325; Abcam, Cambridge, UK). After 3 washes in washing buffer, oocytes were incubated with Alexa Fluor 546-conjugated or Alexa Fluor 488-conjugated goat anti-rabbit IgG (1:200), Alexa Fluor 488-conjugated donkey anti-mouse IgG (1:200), and Alexa Fluor 568-conjugated rabbit anti-goat IgG (1:200) for 1 h at RT. After 3 washes, oocytes were incubated for 5 min with Hoechst 33,342 dye (5 µg/mL) prepared in D-PBS. Finally, oocytes were mounted onto glass slides and examined using a laser scanning confocal microscope (Zeiss LSM 710 META, Oberkochen, Germany). Images were analyzed using the ImageJ software (National Institutes of Health, Bethesda, MD).

Table 1 Primers used in the RT-PCR

Gene	Gene ID	Direction	Sequence (5′–3′)	Size (bp)
AREG	NM_214376.1	F	CACCATGGTCCACAGCGATT	142
		R	AGCTGCACCTTCATATTCCC	
COX2	NM_214321.1	F	CGAGGACCAGCTTTCACCAA	162
		R	AGTGTCTTTGGCTGTCGGAG	
PTX3	NM_001244783.1	F	AACGGTGACCTGATAGCCAC	107
		R	CCACCCACACAGCATCCATT	
HAS2	NM_214053.1	F	TGAGTCTGGGCTATGCAACA	101
		R	GCATTGTACAGCCACTCTCG	

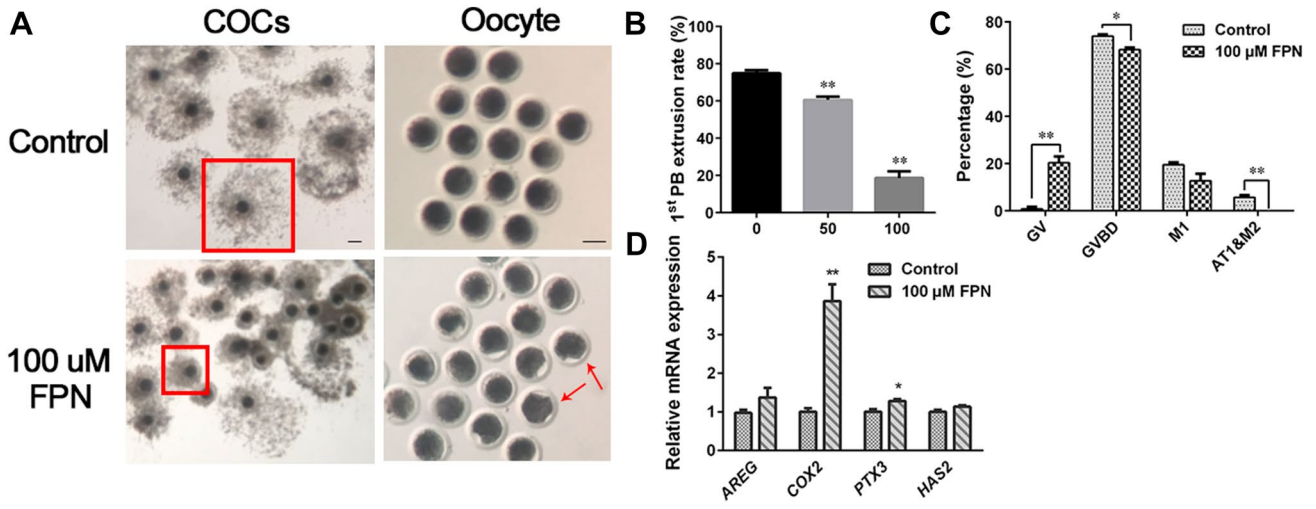

Fig. 1 Effects of fipronil (FPN) on first polar body extrusion rate, cell cycle in porcine oocytes, and cumulus cell expansion gene expression. **a** Porcine COCs were cultured with 0, 50, and 100 μM FPN for 44 h. Only the 0 and 100 μM FPN-treated groups were shown. Cumulus cell expansion decreased (red rectangles) and the morphology of oocytes changed (red arrows) after FPN exposure. Bar = 100 μm. **b** The first polar body extrusion rate significantly decreased after FPN treatment for 44 h. control, n = 361; 50 μM FPN-treated group, n = 325; 100 μM FPN-treated group, n = 301. **c** Cell cycle analysis of oocytes cultured with 0 or 100 μM FPN for 28 h. **d** Quantitative analysis of the effect of FPN on the expansion of cumulus cells. Statistically significant differences are indicated by asterisks (*$p < 0.05$ and **$p < 0.01$) (Color figure online)

Colocalization assay of mitochondria and cytochrome C

To investigate the colocalization of mitochondria and cytochrome C, oocytes were incubated with 500 nM MitoTracker Red CMXRos (Cat #M7512, Invitrogen, Eugene, OR, USA) at 38.5 °C for 30 min. After three washes with PBS-PVA, staining of cytochrome C was carried out as described in "Immunofluorescence staining" section.

Western blotting

For Western blotting, 200 oocytes and cumulus cells were collected in SDS sample buffer and heated for 5 min at 95 °C. Proteins were separated by SDS-PAGE and electrically transferred to polyvinylidene fluoride membranes. Membranes were blocked in Tris-buffered saline containing Tween 20 (TBST) containing 5% BSA for 1 h and then incubated overnight at 4 °C with the primary antibody (1:1000). The primary antibodies used were rabbit anti-P53 (Cat: #sc6243, Santa Cruz), rabbit anti-P21 (Cat: #ab18209, Abcam) and mouse anti-β-actin (Cat: #ab6276, Abcam) antibodies. After washing three times in TBST (each for 10 min), membranes were incubated for 1 h at 37 °C with a peroxidase-conjugated secondary antibody (1: 2000; Cat: #GTX213110-01 and GTX213111-01, Gene Tex). Finally, membranes were processed using SuperSignal West Femto Maximum Sensitivity Substrate (Thermo Scientific, Waltham, MA, USA).

Time-lapse microscopy for chromatin tracking and cyclin B1 activity monitoring

To visualize chromosomes and cyclin B1 activity, the oocytes were microinjected with H2B-mCherry and cyclin B1-GFP cRNA (1000 ng/μL). Images were captured automatically every 15 min for 24 h by using an inverted microscope (Lumascope 620; Etaluma Inc., Carlsbad, CA, USA) installed in an incubator with an atmosphere of 5% CO_2 and maintained at 38.5 °C.

CDK1 kinase assay

Oocytes were collected at 20 h, 24 h, and 28 h of IVM for CDK1 activity detection around GVBD (24 h of IVM). In vitro Cyclin-dependent kinase 1 (CDK1) activity was quantified with the MESACUP® CDC2/CDK1 Kinase Assay Kit (Cat: #5234; MBL, Nagoya, Japan) according to previously reported methods [33]. Briefly, 5 μL of oocyte extract (containing 20 oocytes) was mixed with 45 μL of kinase assay buffer, 10% MV peptide solution (w/v; SLYSSPGGAYC, MBL), 0.1 mM adenosine triphosphate (ATP). The mixture was incubated for 30 min at 30 °C. The reaction was terminated with 200 μL PBS (pH 7.5) containing 50 mM ethylene glycol tetra-acetic acid (EGTA). Phosphorylation of MV peptides was detected by an enzyme linked immunosorbent assay (ELISA). Values were expressed as optical densities (OD) from experiments performed in triplicate.

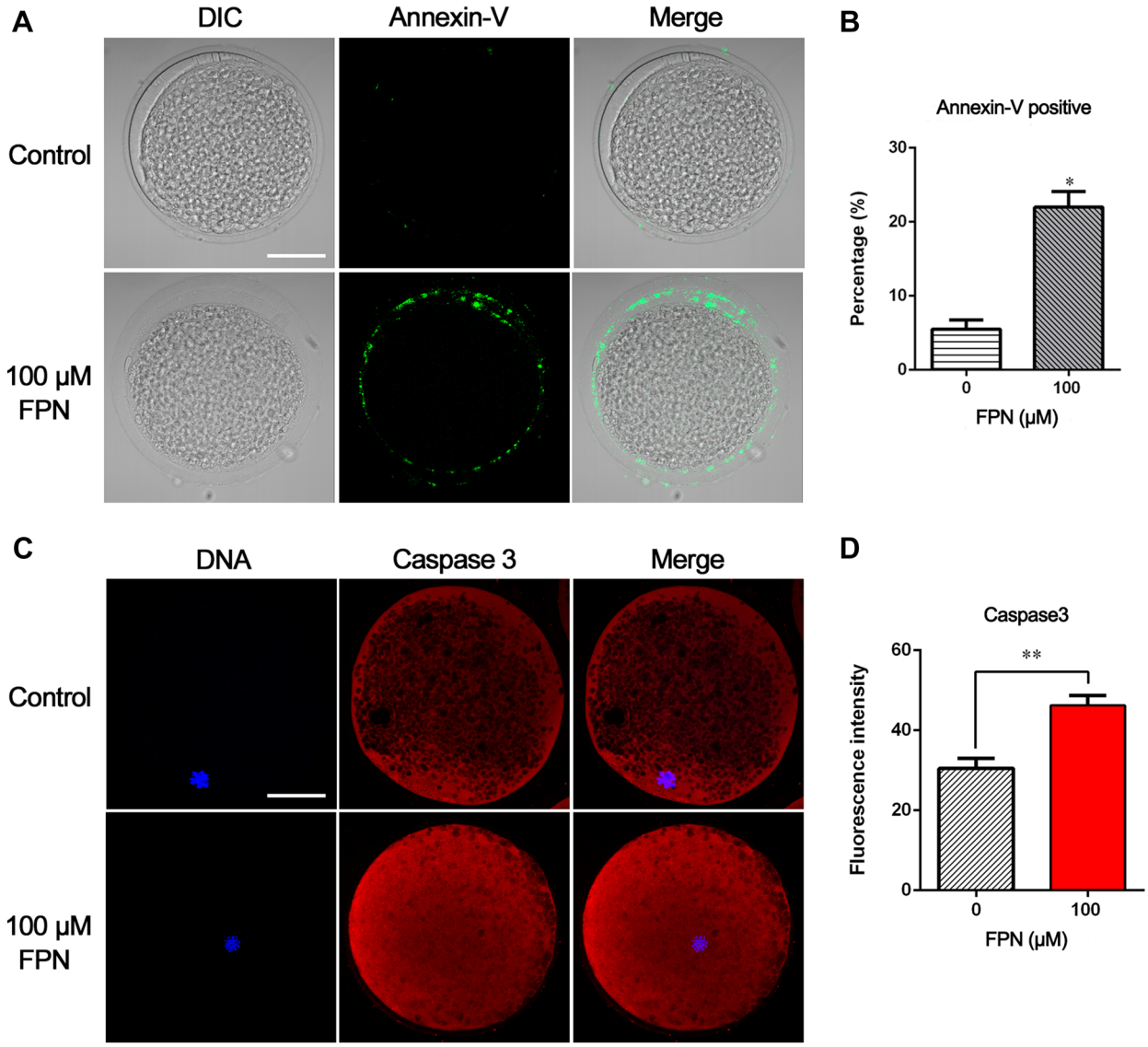

Fig. 2 Effect of fipronil (FPN) on apoptosis and autophagy in porcine oocytes. **a** FPN induced early stage apoptosis among meiosis II oocytes. In the control group, normal oocytes exhibited fluorescence on the zona, whereas oocytes in early apoptosis exhibited fluorescence on the zona and cell membrane. Bar = 50 μm. **b** The early apoptosis rate in the FPN-treated group was significantly increased. Control, n = 62; 100 μM FPN-treated group, n = 65. **c** Representative images of caspase 3 (red) expression in the control and FPN-treated groups. Bar = 50 μm. **d** The expression levels of caspase 3 was significantly higher in the 100 μM FPN-treated group compared to the control. Control: n = 48; 100 μM FPN-treated group, n = 40. Statistically significant differences are indicated by asterisks (*$p < 0.05$ and **$p < 0.01$) (Color figure online)

Statistical analysis

All data were analyzed by one-way analysis of variance and *t* test with SPSS software (SPSS, Inc., Chicago, IL, USA). Differences among the treatments were examined by the Duncan multiple range test. Data are expressed as the mean ± standard error of the mean. Each experiment was performed in triplicate, and differences were considered significant when $p < 0.05$.

Results

FPN impede oocyte maturation and cumulus cell expansion

The COCs were cultured in different concentrations of FPN for 44 h. First, the extent of cumulus cells expansion was weaker in the 100 μM FPN treatment group compared with the control group (Fig. 1a). Amphiregulin (AREG) is an epidermal growth factor (EGF)-like peptide promoting the

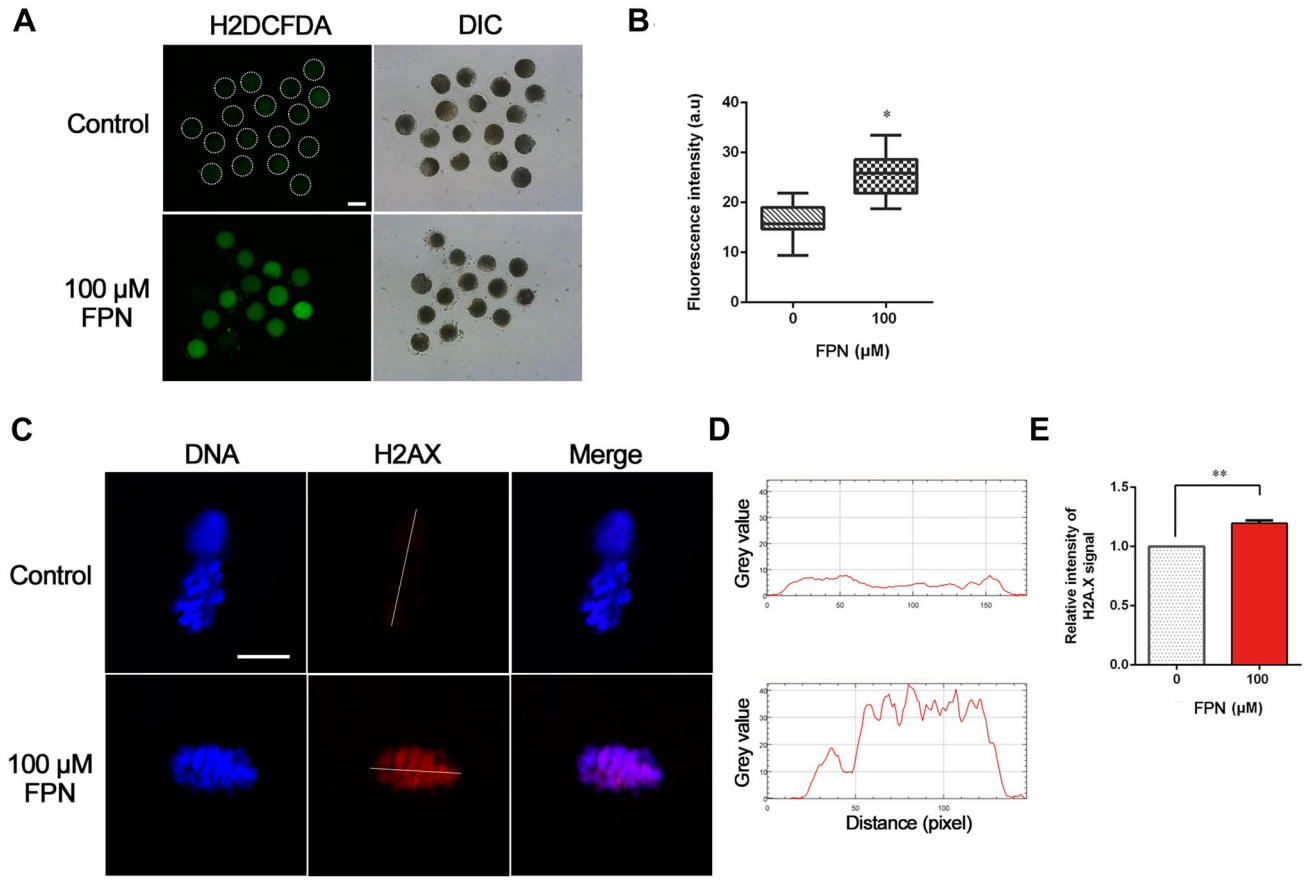

Fig. 3 Intracellular changes occur among porcine oocytes treated with fipronil (FPN). **a** FPN effect on ROS generation determined by H_2DCFDA fluorescence (green) in porcine oocytes. Bar = 100 μm. **b** The fluorescence intensity was significantly increased after the 100 μM FPN treatment. Control, n = 62; 100 μM FPN-treated group, n = 65. **c** Representative images of chromosomes stained with γH2AX (red) in control and FPN-treated groups. Bar = 10 μm. The linear intensities of γH2AX levels on the chromosomes from control and FPN-treated groups were analyzed and shown in **d**. **e** The expression of γH2AX on the chromosomes significantly increased after the 100 μM FPN treatment. Control, n = 42; 100 μM FPN-treated group, n = 38. Statistically significant differences are indicated by asterisks (*p < 0.05 and **p < 0.01) (Color figure online)

oocyte maturation and expansion of cumulus cells. Cyclooxygenase 2 (*COX2*), hyaluronic acid synthase 2 (*HAS2*) and pentraxin 3 (*PTX3*) are downstream of *GDF9*, and expression of these genes is closely related to cumulus cell expansion [36, 37]. In contrast to the inhibited expansion of cumulus cells, the *COX2* and *PTX3* expression significantly increased in the 100 μM FPN treated group (Fig. 1d). In addition, the first polar body extrusion rates in the 50 μM (60.55 ± 1.48%; Fig. 1b) and 100 μM (18.64 ± 2.95%, Fig. 1b) FPN groups were significantly lower than those in the control group (74.90 ± 1.50%; Fig. 1b). Therefore, the 100 μM concentration was chosen for subsequent experiments. Next, cell cycle analysis was performed after 28 h of IVM. The percentage of GV stage oocytes were significantly higher in the 100 μM FPN group (20.38 ± 2.19% vs. 0.83 ± 0.68%, p < 0.01, Fig. 1c). However, the percentages of GVBD stage (68.22 ± 0.79% vs. 73.97 ± 0.62%, p < 0.05, Fig. 1c) and AT1&M2 stage (0% vs. 20.38 ± 0.73%, p < 0.01, Fig. 1c) oocytes from the 100 μM FPN group were significantly lower than those from the control group.

FPN caused enhanced apoptosis in porcine oocytes

The Annexin-V positive rate in the 100 μM FPN group was significantly higher than the control group (Fig. 2a, b; p < 0.05). Next, the expression of CASP3 was detected and increased significantly in the 100 μM FPN group (Fig. 2c, d; p < 0.01).

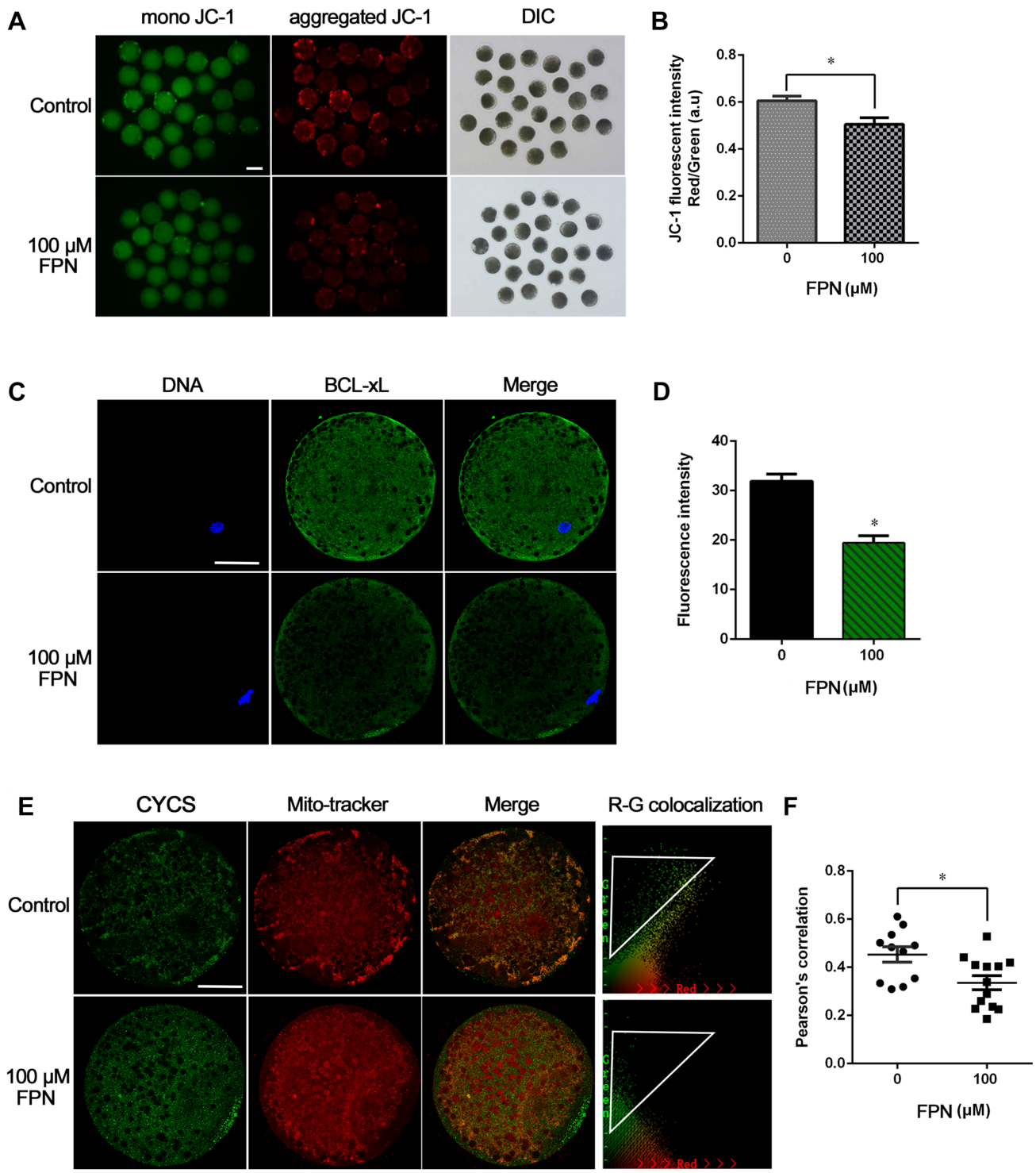

Fig. 4 Fipronil (FPN) impaired mitochondrial function. **a** Representative images of mono JC-1 (green) and aggregated JC-1 (red) fluorescence in control and fipronil (FPN)-treated groups. Bar = 100 µm. **b** The ratio of aggregated JC-1 per mono JC-1 significantly decreased in the 100 µM FPN-treated group compared to the control group. Control, n = 68; 100 µM FPN-treated group, n = 71. **c** Representative images of BCL-xL (green) expression in the control and FPN-treated groups. Bar = 50 µm. **d** The intensity of BCL-xL significantly decreased after the 100 µM FPN treatment ($p < 0.05$). Control, n = 42; 100 µM FPN-treated group, n = 45. **e** Representative images of cytochrome C (CYCS, green) and MitoTracker (red) expression in the control and FPN-treated groups. The colocalization of CYCS and MitoTracker is shown. Bar = 50 µm. **f** The Pearson correlation coefficient between CYCS and mitochondria significantly decreased after the 100 µM FPN treatment ($p < 0.05$). Control, n = 14; 100 µM FPN-treated group, n = 15. Statistically significant differences are indicated by asterisks (*$p < 0.05$ and **$p < 0.01$) (Color figure online)

Increased ROS levels and DNA damage were found after FPN treatment

To explore the mechanism for the apoptosis and cell cycle arrest, ROS levels and DNA damage were examined. The ROS levels in the 100 μM FPN group were significantly higher than those in the control group (Fig. 3a, b; $p < 0.05$). Furthermore, the γH2AX signal on the chromosomes of the 100 μM FPN group was significantly higher than that in the control group (Fig. 3c, d and e; $p < 0.01$).

High concentrations of FPN has an adverse effect on mitochondria function

First, the mitochondrial membrane potential was detected. The aggregated JC-1/mono JC-1 ratio in the 100 μM FPN group was significantly lower than the control group, which indicated an increase in membrane permeability (Fig. 4a, b; $p < 0.05$). Next, the expression of the anti-apoptosis protein Bcl-xL was detected. The intensity of Bcl-xL in the 100 μM FPN group dropped significantly (Fig. 4c, d; $p < 0.05$). Lastly, a mitochondria-cytochrome C colocalization analysis was carried out. Compared to the control group, the 100 μM FPN group showed reduced colocalized signal and the Pearson correlation coefficient was lower (Fig. 4e, f; $p < 0.05$).

FPN induced cell cycle arrest in porcine oocytes

To investigate the pathway activated by the DNA damage by assessing the expression of the ataxia telangiectasia-mutated (ATM) protein. Phosphorylated ATM in the 100 μM FPN group significantly increased in the chromosome and cytoplasm compared to the control group (Fig. 5a, b; $p < 0.05$). Subsequently, the expression of the cell cycle protein CDK1 was assessed, and the result showed that inactivated CDK1 (tyrosine 15 phosphorylated) significantly increased in the 100 μM FPN group compared with the control group (Fig. 5c, d; $p < 0.05$). The P53 and P21 protein expression were detected by western blotting, and the expression level of P53 and P21 both significantly increased in the 100 μM FPN group oocytes, and the expression level of P53 significantly increased in the 100 μM FPN group cumulus cells (Fig. 5e–h; $p < 0.05$).

FPN impeded porcine oocyte GVBD by inhibiting CDK1 activity

At the beginning, time-lapse was employed to observe the cyclin B1 degradation. We observed that cyclin B1 degradation in the 100 μM FPN group was delayed (Fig. 6a, b). The CDK1 activity is related to G2/M transition, which rapidly increases during GVBD (approximately 24 h of IVM), and GV arrest appears when CDK1 activity is inhibited [38]. Hence, the CDK1 activity during GVBD was examined from 20 to 28 h, which showed significant lower MPF activity after 20 h of IVM and a delayed increase in the 100 μM FPN group compared with the control (Fig. 6c; $p < 0.05$).

Fig. 5 Cell cycle arrest caused by DNA damage through the ATM pathway. **a** Representative images of phosphorylated-ATM (red) expression in the control and fipronil (FPN)-treated groups. Bar = 100 μm. **b** The intensity of ATM significantly increased after the 100 μM FPN treatment ($p < 0.01$). Control, n = 35; 100 μM FPN-treatment group, n = 38. **c** Representative images of phosphorylated-CDK1 (Tyr15, red) expression in the control and FPN-treated groups. Bar = 50 μm. **d** The intensity of phosphorylated-CDK1 significantly increased after the 100 μM FPN treatment ($p < 0.01$). Control, n = 61; 100 μM FPN-treated group, n = 58. **e** Western blotting result of P53 or P21 from control and 100 μM FPN-treated group were shown. Oocyte (OO): Control, n = 200; 100 μM FPN-treated group, n = 200. All experiments were carried out in triplicate. Quantitation and statistical analyses of **e** are shown in **f**, **g** and **h**. CCs: cumulus cells. ACTB: β-actin. TUBB: β-tubulin. Statistically significant differences are indicated by asterisks (*$p < 0.05$ and **$p < 0.01$) (Color figure online)

Discussion

The chiral insecticide, FPN, had been extensively used on cotton, rice, and corn crops as well as in commercial grass management and residential pest control for the past 20 years. Although people have benefited from the use of FPN, it is still risky to use in the farm. Previous studies have demonstrated adverse effects of FPN on mammalian somatic cells and the male reproductive system [5, 7, 16]. Although a recent study showed that FPN impeded mouse preimplantation embryo development [39], no studies about the effect of FPN on mammalian oocyte maturation have been reported. Furthermore, a maternal transfer of FPN to the next generation has been reported in zebrafish [40]. Therefore, it is important to find out whether the application of FPN in pig farm will cause adverse effect on sow's reproductive system and the mechanism underneath. In the present study, it was observed that 100 μM of FPN harms the porcine oocytes by inducing excessive ROS and DNA damage during in vitro maturation. Therefore, FPN could have a potential toxicity on porcine oogenesis and may be harmful to reproduction of sows.

FPN can induce excessive ROS in rat sperms and human SH-SY5Y neuronal cells [5, 7, 14]. As we know, ROS are usually derived from mitochondria respiratory activity, which includes hydrogen peroxide (H_2O_2) and superoxide (O_2^-) [18]. The excessive ROS perturb oogenesis because oocytes are susceptible to these molecules [41]. The oocytes of pigs have large amounts of lipids, which are sensitive to ROS [42]. In this study, H2DCFDA, an ROS indicator, showed higher ROS levels in the 100 μM FPN-treated group.

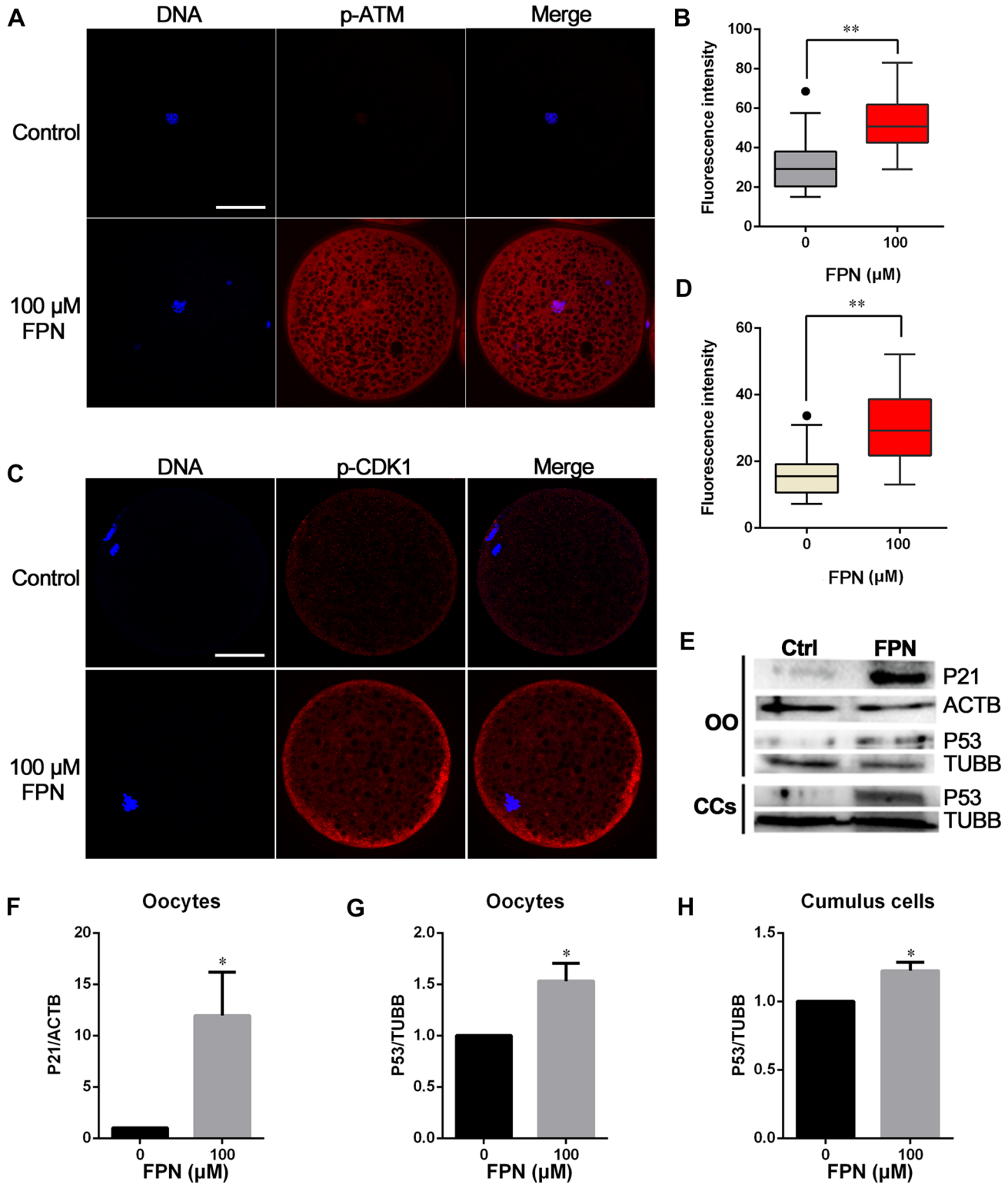
A
DNA
p-ATM
Merge
Control
100 μM FPN
B
Fluorescence intensity
FPN (μM)
**
C
DNA
p-CDK1
Merge
Control
100 μM FPN
D
Fluorescence intensity
FPN (μM)
**
E
Ctrl
FPN
OO
P21
ACTB
P53
TUBB
CCs
P53
TUBB
F
Oocytes
P21/ACTB
FPN (μM)
G
Oocytes
P53/TUBB
FPN (μM)
H
Cumulus cells
P53/TUBB
FPN (μM)

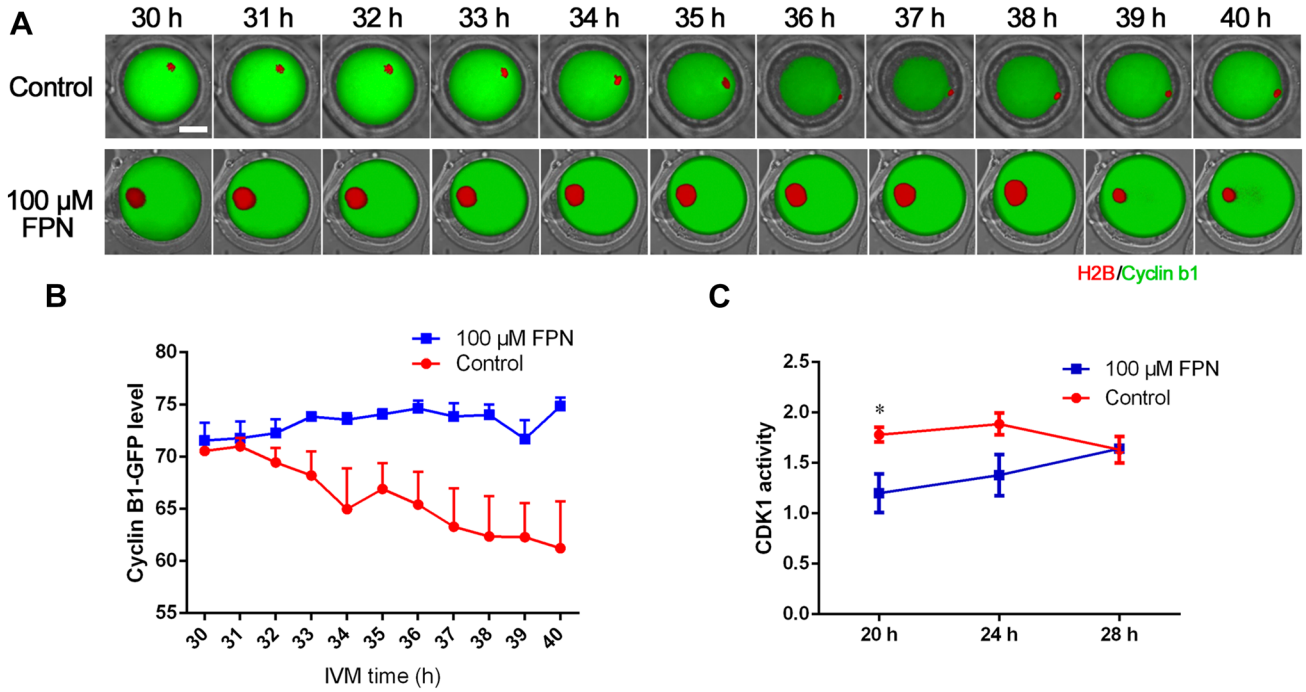

Fig. 6 Effect of fipronil (FPN) on cyclin B1 degradation and CDK1 activity. **a** Time-lapse images of oocytes injected with H2B-mcherry (red) and cyclin B1-GFP (green) cultured in 0 and 100 μM FPN. Bar = 50 μm. **b** The cyclin B1-GFP level of control (red) and 100 μM FPN-treated group (blue) were detected by time-lapse imaging during in vitro maturation (IVM), **c** CDK1 activity was detected during GVBD. The activity of CDK1 in the FPN-treated group (blue) was significantly lower than that of the control group (red, $p < 0.05$) at 20 h of IVM. Control, n = 60; 100 μM FPN-treated group, n = 60 (Color figure online)

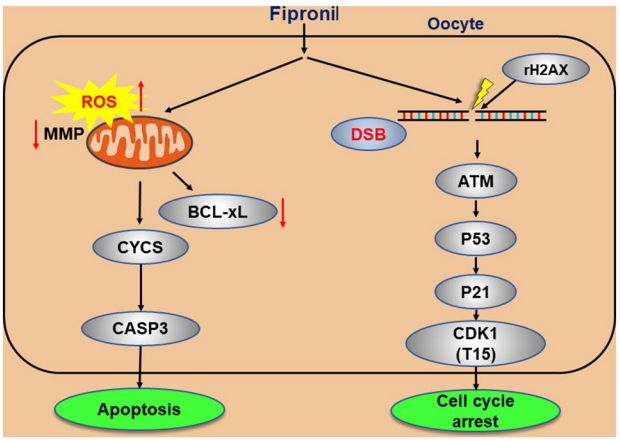

Fig. 7 Summary of the effect of fipronil (FPN) on porcine oocyte maturation. The FPN caused excessive generation of reactive oxygen species (ROS), decrease of mitochondrial membrane potential and DNA damage. Further, mitochondrial dysfunction and DNA damage led to apoptosis and cell cycle arrest

ROS can increase the expression of pro-apoptotic genes (*Bax*, *Caspase3*) and inhibit the expression of pro-survival genes (*Bcl-2*, *Bcl-xL*). Moreover, ROS disrupt the mitochondrial membrane potential and reduce ATP levels, and then the decreased mitochondrial membrane potential might lead to the release of cytochrome C from the mitochondria into the cytoplasm [43, 44]. Subsequently, the increased cytoplasmic cytochrome C levels would activate Caspase-9 and Caspase-3, which eventually leads to apoptosis. The results showed that FPN led to a decrease in Bcl-xL levels, release of cytochrome C, and an enhancement of Caspase3 activity, suggesting that excessive ROS caused by FPN might be the cause of impaired mitochondrial function, which needs to be further investigated.

DNA damage can induce apoptosis and cell cycle arrest [25, 45]. Cell cycle arrest because of DNA damage has been hypothesized to be a self-saving mechanism to provide enough time for repairing the DNA lesions. It has been reported that FPN intake resulted in micronuclei in the peripheral blood of mice as well as DNA damage in human blood lymphocytes [17, 46]. In the present study, 100 μM FPN treatment induced a significantly higher level of DNA damage as indicated by γH2AX, a marker for DNA strand break [47]. A previous study has shown that oocytes arrested at the G2–M stage (GV stage arrest) when DNA lesions occur [48]. Additionally, cyclin B1 is the principal molecule for regulation in pig oocyte maturation [49], and the amount of cyclin B indicates MPF activity in oocytes, which significantly decreases between the meiosis I and II stages [26]. In the present study, the DNA damage caused the activation of ATM pathway, and a delayed

degradation of cyclin b1 as well as the low CDK1 activity. The pathway regulating CDK1 activity includes Chk1/Chk2-Cdc25c and P53-P21 [30, 31, 50]. In the present study, FPN treatment activated the ATM-P53-P21 pathway, which is consistent with previous results. This suggested that FPN could possibly cause GV stage arrest in porcine oocytes because of DNA damage, which blocked porcine oocytes from further development.

Intriguingly, the increase in *COX2* and *PTX3* mRNA levels was in contradiction to the inhibited cumulus expansion. Overexpression of *COX2* and tumor necrosis factor-α (*TNF-α*) has been reported in SH-SY5Y cells after 100 μM FPN treatment [51], which indicated FPN could induce inflammatory response in neuronal cells. *PTX3* was expressed rapidly when primary inflammatory signals (for example, TNFα) occurred [52]. FPN could also cause the activation of MAPK pathway and induce accumulation of nuclear P53, which finally causes apoptosis [51]. Therefore, 100 μM FPN might induce inflammatory response in the cumulus cells and cause apoptosis before the expansion of cumulus cells.

In conclusion, FPN can accelerate ROS production inside the porcine oocytes and increase the extent of DNA damage. FPN also induced apoptosis because of mitochondrial dysfunction. Furthermore, the DNA damage led to a GV stage arrest and a delayed cell cycle by inhibition of MPF activity (Fig. 7). Overall, these results demonstrated that FPN has a detrimental effect on the porcine oocyte maturation and could impair the reproduction performance of sows when pesticides including FPN was used around the pig farm. It needs to be further investigated if the FPN will accumulate inside the sows and if its toxicity will be transferred to next generation.

Acknowledgement This research was supported by Basic Science Research Program through the National Research Foundation of Korea (NRF) funded by the Ministry of Education (No. 2018R1A2B6001173), Republic of Korea. Also, I would like to thank Doctor Namgoong for providing cyclin B1-GFP and H2B-mCherry expression plasmid.

Compliance with ethical standards

Conflict of interest We declare that we have no conflict of interest.

References

1. Konwick BJ, Fisk AT, Garrison AW, Avants JK, Black MC (2005) Acute enantioselective toxicity of fipronil and its desulfinyl photoproduct to *Ceriodaphnia dubia*. Environ Toxicol Chem 24:2350–2355
2. Varró P, Gyori J, Világi I (2009) In vitro effects of fipronil on neuronal excitability in mammalian and molluscan nervous systems. Ann Agric Environ Med 16:71–77
3. Vidau C, Brunet J-L, Badiou A, Belzunces LP (2009) Phenylpyrazole insecticides induce cytotoxicity by altering mechanisms involved in cellular energy supply in the human epithelial cell model Caco-2. Toxicol In Vitro 23:589–597
4. Das PC, Cao Y, Cherrington N, Hodgson E, Rose RL (2006) Fipronil induces CYP isoforms and cytotoxicity in human hepatocytes. Chem Biol Interact 164:200–214
5. Ki Y-W, Lee JE, Park JH, Shin IC, Koh HC (2012) Reactive oxygen species and mitogen-activated protein kinase induce apoptotic death of SH-SY5Y cells in response to fipronil. Toxicol Lett 211:18–28
6. Leghait J, Gayrard V, Picard-Hagen N et al (2009) Fipronil-induced disruption of thyroid function in rats is mediated by increased total and free thyroxine clearances concomitantly to increased activity of hepatic enzymes. Toxicology 255:38–44
7. Khan S, Jan M, Kumar D, Telang A (2015) Firpronil induced spermotoxicity is associated with oxidative stress, DNA damage and apoptosis in male rats. Pestic Biochem Physiol 124:8–14
8. Stehr CM, Linbo TL, Incardona JP, Scholz NL (2006) The developmental neurotoxicity of fipronil: notochord degeneration and locomotor defects in zebrafish embryos and larvae. Toxicol Sci 92:270–278
9. Qureshi IZ, Bibi A, Shahid S, Ghazanfar M (2016) Exposure to sub-acute doses of fipronil and buprofezin in combination or alone induces biochemical, hematological, histopathological and genotoxic damage in common carp (*Cyprinus carpio* L.). Aquat Toxicol 179:103
10. Banerjee BD, Seth V, Ahmed RS (2001) Pesticide-induced oxidative stress: perspective and trends. Rev Environ Health 16:1–40
11. Miranda MD, de Bruin VM, Vale MR, Viana GS (2000) Lipid peroxidation and nitrite plus nitrate levels in brain tissue from patients with Alzheimer's disease. Gerontology 46:179–184
12. Dumollard R, Carroll J, Duchen MR, Campbell K, Swann K (2009) Mitochondrial function and redox state in mammalian embryos. Semin Cell Dev Biol 20:346–353
13. Gupta S, Sekhon L, Kim Y, Agarwal A (2010) The role of oxidative stress and antioxidants in assisted reproduction. Curr Womens Health Rev 6:227–238
14. Lee JE, Kang JS, Ki Y-W et al (2011) Akt/GSK3β signaling is involved in fipronil-induced apoptotic cell death of human neuroblastoma SH-SY5Y cells. Toxicol Lett 202:133–141
15. de Castilhos Ghisi N, Ramsdorf WA, Ferraro MVM, de Almeida MIM, de Oliveira Ribeiro CA, Cestari MM (2011) Evaluation of genotoxicity in Rhamdia quelen (Pisces, Siluriformes) after sub-chronic contamination with Fipronil. Environ Monit Assess 180:589–599
16. Girgis SM, Yassa VF (2013) Evaluation of the potential genotoxic and mutagenic effects of fipronil in rats. J Mediterr Ecol 12:5–11
17. Çelik A, Ekinci SY, Güler G, Yildirim S (2014) In vitro genotoxicity of fipronil sister chromatid exchange, cytokinesis block micronucleus test, and comet assay. DNA Cell Biol 33:148–154
18. Balaban RS, Nemoto S, Finkel T (2005) Mitochondria, oxidants, and aging. Cell 120:483–495
19. Chen D, Li X, Liu X et al (2017) NQO2 inhibition relieves ROS effects on mouse oocyte meiotic maturation and embryo development. Biol Reprod 97:598–611
20. Luberda Z (2005) The role of glutathione in mammalian gametes. Reprod Biol 5:5–17
21. Bedaiwy MA, Elnashar SA, Goldberg JM et al (2012) Effect of follicular fluid oxidative stress parameters on intracytoplasmic sperm injection outcome. Gynecol Endocrinol 28:51–55
22. Palini S, Benedetti S, Tagliamonte MC et al (2014) Influence of ovarian stimulation for IVF/ICSI on the antioxidant defence system and relationship to outcome. Reprod Biomed Online 29:65–71

23. Orrenius S, Gogvadze V, Zhivotovsky B (2007) Mitochondrial oxidative stress: implications for cell death. Annu Rev Pharmacol Toxicol 47:143–183
24. Clarke PG, Clarke S (1995) Historic apoptosis. Nature 378:230
25. Elledge SJ (1996) Cell cycle checkpoints: preventing an identity crisis. Science 274:1664–1672
26. Nebreda AR, Ferby I (2000) Regulation of the meiotic cell cycle in oocytes. Curr Opin Cell Biol 12:666–675
27. Choi W-J, Banerjee J, Falcone T, Bena J, Agarwal A, Sharma RK (2007) Oxidative stress and tumor necrosis factor–α–induced alterations in metaphase II mouse oocyte spindle structure. Fertil Steril 88:1220–1231
28. Tamura H, Takasaki A, Miwa I et al (2008) Oxidative stress impairs oocyte quality and melatonin protects oocytes from free radical damage and improves fertilization rate. J Pineal Res 44:280–287
29. Sugino N (2005) Reactive oxygen species in ovarian physiology. Reprod Med Biol 4:31–44
30. Bolcunfilas E, Rinaldi VD, White ME, Schimenti JC (2014) Reversal of female infertility by Chk2 ablation reveals the oocyte DNA damage checkpoint pathway. Science 343:533–536
31. Kastan MB, Onyekwere O, Sidransky D, Vogelstein B, Craig RW (1991) Participation of p53 protein in the cellular response to DNA damage. Cancer Res 51:6304–6311
32. De Oliveira PR, Bechara GH, Denardi SE, Oliveira RJ, Mathias MIC (2012) Cytotoxicity of fipronil on mice liver cells. Microsc Res Tech 75:28–35
33. Han J, Wang Q-C, Zhu C-C et al (2016) Deoxynivalenol exposure induces autophagy/apoptosis and epigenetic modification changes during porcine oocyte maturation. Toxicol Appl Pharmacol 300:70–76
34. Zhang Y, Han J, Zhu C-C et al (2016) Exposure to HT-2 toxin causes oxidative stress induced apoptosis/autophagy in porcine oocytes. Sci Rep 6:33904
35. Kitajima TS, Ohsugi M, Ellenberg J (2011) Complete kinetochore tracking reveals error-prone homologous chromosome biorientation in mammalian oocytes. Cell 146:568–581
36. Prochazka R, Petlach M, Nagyova E, Němcová L (2011) Effect of epidermal growth factor-like peptides on pig cumulus cell expansion, oocyte maturation, and acquisition of developmental competence in vitro: comparison with gonadotropins. Reproduction 141:425–435
37. Varani S, Elvin JA, Yan C et al (2002) Knockout of pentraxin 3, a downstream target of growth differentiation factor-9, causes female subfertility. Mol Endocrinol 16:1154–1167
38. Oqani RK, Lin T, Lee JE, Kim SY, Kang JW, Jin DI (2017) Effects of CDK inhibitors on the maturation, transcription, and MPF activity of porcine oocytes. Reprod Biol 17:320–326
39. Šefčíková Z, Babeľová J, Čikoš Š et al (2018) Fipronil causes toxicity in mouse preimplantation embryos. Toxicology 410:214–221
40. Xu C, Niu L, Liu J et al (2019) Maternal exposure to fipronil results in sulfone metabolite enrichment and transgenerational toxicity in zebrafish offspring: indication for an overlooked risk in maternal transfer? Environ Pollut 246:876–884
41. Chaube SK, Prasad PV, Thakur SC, Shrivastav TG (2005) Hydrogen peroxide modulates meiotic cell cycle and induces morphological features characteristic of apoptosis in rat oocytes cultured in vitro. Apoptosis 10:863–874
42. Han J, Wang T, Fu L et al (2015) Altered oxidative stress, apoptosis/autophagy, and epigenetic modifications in Zearalenone-treated porcine oocytes. Toxicol Res 4:1184–1194
43. Liu X, Kim CN, Yang J, Jemmerson R, Wang X (1996) Induction of apoptotic program in cell-free extracts: requirement for dATP and cytochrome c. Cell 86:147–157
44. Tsujimoto Y, Shimizu S, Eguchi Y, Kamiike W, Matsuda H (1997) Bcl-2 and Bcl-xL block apoptosis as well as necrosis: possible involvement of common mediators in apoptotic and necrotic signal transduction pathways. Leukemia 11(Suppl 3):380–382
45. Lin F, Ma XS, Wang ZB et al (2014) Different fates of oocytes with DNA double-strand breaks in vitro and in vivo. Cell Cycle 13:2674
46. de Oliveira PR, Bechara GH, Denardi SE, Oliveira RJ, Mathias MI (2012) Genotoxic and mutagenic effects of fipronil on mice. Exp Toxicol Pathol 64:569–573
47. Valdiglesias V, Giunta S, Fenech M, Neri M, Bonassi S (2013) γH2AX as a marker of DNA double strand breaks and genomic instability in human population studies. Res Rev Mutat Res 753:24–40
48. Marangos P, Carroll J (2012) Oocytes progress beyond prophase in the presence of DNA damage. Curr Biol 22:989–994
49. Kuroda T, Naito K, Sugiura K, Yamashita M, Takakura I, Tojo H (2004) Analysis of the roles of Cyclin B1 and Cyclin B2 in porcine oocyte maturation by inhibiting synthesis with antisense RNA injection1. Biol Reprod 70:154–159
50. Karlsson-Rosenthal C, Millar J (2006) Cdc25: mechanisms of checkpoint inhibition and recovery. Trends Cell Biol 16:285
51. Park JH, Park YS, Lee JB et al (2016) Meloxicam inhibits fipronil-induced apoptosis via modulation of the oxidative stress and inflammatory response in SH-SY5Y cells. J Appl Toxicol 36:10–23
52. Han B, Mura M, Andrade CF et al (2005) TNFα-induced long pentraxin PTX3 expression in human lung epithelial cells via JNK. J Immunol 175:8303–8311